

CORROSION BEHAVIOUR OF COMPOSITE COATINGS OBTAINED BY ELECTROLYTIC CODEPOSITION OF ZINC WITH NANOPARTICLES OF $\text{CeO}_2\cdot\text{ZrO}_2$ BINARY OXIDES

PATRICK IOAN NEMES^a, NICOLETA COTOLAN^a,
LIANA MARIA MURESAN^{a*}

ABSTRACT. Composite Zn coatings incorporating $\text{CeO}_2\cdot\text{ZrO}_2$ nanoparticles were obtained by electrodeposition on steel from an industrial electrolyte, containing 75 g L^{-1} ZnCl_2 , 230 g L^{-1} KCl , 20 g L^{-1} H_3BO_3 and two additives, 1 mL L^{-1} each.

The influence of the oxide nanoparticles on phase composition, morphology and structure of the obtained coatings was investigated by X-ray diffraction and SEM-EDX methods. By using polarization measurements, the corrosion behaviour of the deposits was examined and the corrosion process on $\text{Zn-CeO}_2\cdot\text{ZrO}_2$ composite coatings was compared with that taking place on composite coatings prepared with a simple mixture of CeO_2 and ZrO_2 oxides and with each oxide separately. On all the composite coatings, corrosion was found to be slower than on the pure Zn surface.

Keywords: Corrosion; Electrodeposition; Zinc-nanoparticles composite coatings; $\text{CeO}_2\cdot\text{ZrO}_2$ binary oxides

INTRODUCTION

The need to improve the corrosion resistance of protective coatings on steel promoted the application of different post plating surface modification treatments (e.g. chrome passivation, protective film generation etc.), but, at the same time, the development of new coatings containing minute amounts of nanoparticles (metal oxides, carbides etc.) with a beneficial effect on the corrosion resistance of the substrate [1].

A survey of recent literature on the metallic composite coatings shows that several oxide nanoparticles are very promising filling dopants for material coatings [2]. Generally, these particles provide improved resistance to oxidation,

^a Department of Chemical Engineering "Babes-Bolyai" University, 1, M. Kogalniceanu St., 400084 Cluj-Napoca, Romania

* Corresponding author: limur@chem.ubbcluj.ro

corrosion, erosion and wear to the composite layer. Consequently, many efforts have been made to include oxidic particles such as TiO_2 , ZrO_2 , CeO_2 , SiO_2 , Al_2O_3 [3–9] etc. into metallic coatings, by using different preparation methods. Among these particles, ZrO_2 and CeO_2 are particularly very interesting due to their promising physical and chemical properties [6, 10, 11].

Thus, zirconia possesses high resistance to wear and corrosion, biocompatibility, heat resistance and presents good adhesion to metallic surfaces [11, 12]. Chemical vapour deposition, electrophoretic deposition and sol–gel deposition by dip coating procedure are common routes to prepare ZrO_2 coatings for anti-corrosion purposes and for the improvement of mechanical properties of the substrates [12, 13]. It was also reported that ZrO_2 nanoparticles can be uniformly co-deposited into a nickel matrix from a Watts bath containing monodispersed particles in suspension, under DC electrodeposition condition [14]. Zn– ZrO_2 composite coatings were also successfully produced by electrodeposition technique from zinc sulphate baths [15]. The electrolytic codeposition of zinc with different micron or submicron size particles suspended in a classical zinc electroplating bath takes place by agitation and/or use of surfactants, at a current density of around 2 A dm^{-2} [3, 16, 17–19].

Cerium oxides and cerium hydroxides are reported as cathodic corrosion inhibitors and have been proposed as effective species for the protection of metals from corrosion. CeO_2 nanoparticles were co-electrodeposited with nickel and conferred the coating enhanced wear and corrosion resistance, microhardness and improved high temperature oxidation resistance [20].

Despite the large number of works published in literature reporting the unique properties of CeO_2 and ZrO_2 , very little has been published about a combination of both in the field of the pre-treatments. It was shown that bis-1,2-[triethoxysilylpropyl]-tetrasulfide silane films containing $\text{CeO}_2\cdot\text{ZrO}_2$ nanoparticles deposited by dip-coating on galvanised steel substrates are very efficient anticorrosion coatings. The presence of zirconium ions provided very good barrier properties, whereas the presence of cerium provided better corrosion inhibition ability [21]. However, to the best of our knowledge, there are no reports on the preparation of composite layers by simultaneous co-deposition of zinc with CeO_2 and ZrO_2 nanoparticles.

In this context, the aim of this work is to investigate the effect of CeO_2 and ZrO_2 nanoparticles, used as a mechanical mixture or as binary $\text{CeO}_2\cdot\text{ZrO}_2$ oxides on the corrosion resistance of zinc coatings, after the electro-co-deposition of nanoparticles with zinc. The method combines the advantages of metal electroplating (such as low cost, versatility and an easy process control) with those of composite materials and allows obtaining advanced materials with tailor-made properties [1].

X ray diffraction (XRD) and SEM-EDX methods were used to determine the structure, the surface morphology and the chemical composition of the deposits. Polarization measurements followed by Tafel interpretation of the polarization curves were carried out in order to characterize the corrosion behaviour of the coatings.

RESULTS AND DISCUSSION

Morphological and structural analysis

SEM observations of the samples (Figures 1, 2) revealed an uniform aspect of the pure Zn deposit, with very small prominences that appear from place to place. The uniformity of the zinc deposit is due mainly to the brightening agents, that reduce the roughness of the surface to a nanometric level.

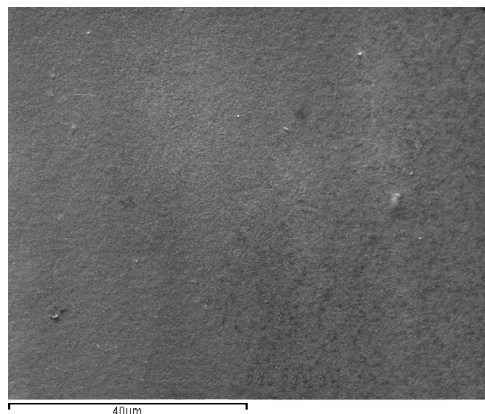


Figure 1. SEM micrograph of pure Zn deposits

In the presence of the $\text{CeO}_2 + \text{ZrO}_2$ mixture in the plating bath, the cathodic deposit becomes more fine grained, but less uniform (Figure 2).

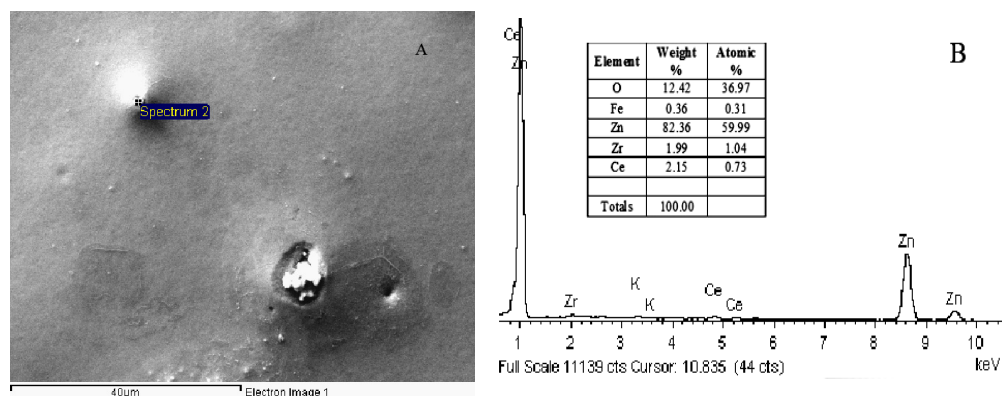


Figure 2. SEM micrograph (A) and EDX spectrum (B) of Zn-($\text{CeO}_2 + \text{ZrO}_2$) deposits

This can be due to the fact that the nanoparticles interfere with the nucleation–growth process by enhancing nucleation and exerting a detrimental effect on the crystal growth. Observations of the Zn–($\text{CeO}_2+\text{ZrO}_2$) composite coating by EDX analysis, performed on the irregularities of the surface (Fig. 2B) revealed the presence of both ceria and zirconia, thus proving the successful incorporation of nanoparticles in the metallic matrix. Nevertheless, a small degree of embedded oxide nanoparticles can be observed (table in Fig. 2B), values that are close to those reported in previous works [5, 6].

X-ray Diffraction

The XRD spectra of the investigated specimens are depicted in Figure 3. The main diffraction line can be attributed to the preferential hexagonal orientation of the zinc crystallites on the (101) direction, mainly determined by the presence of surfactants in the plating bath. It has been suggested that a preferred orientation of the zinc crystallites to the (101) direction may facilitate a good co-deposition of ceria [22], and possibly of other nanoparticles as well.

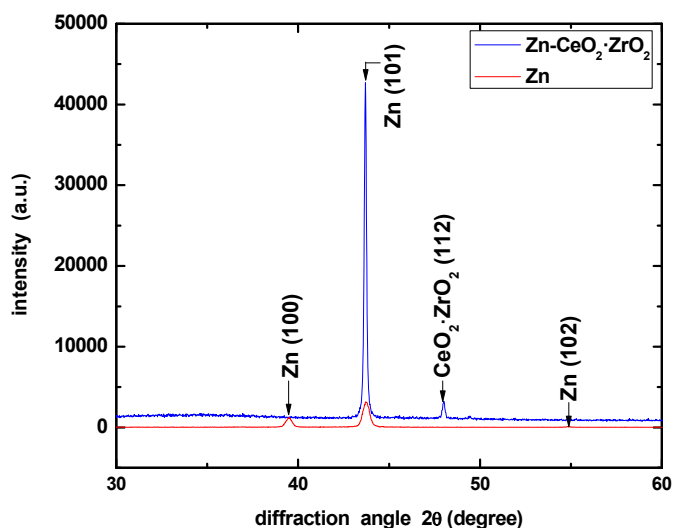


Figure 3. X-ray Diffraction results for the Zn and Zn- $\text{CeO}_2\cdot\text{ZrO}_2$ deposits, 1.25 g L^{-1}

Upon addition of the $\text{CeO}_2\cdot\text{ZrO}_2$ oxide nanoparticles in the electrolytic bath, the diffraction lines of the resulting deposits exhibit a change in intensity, indicating a textural modification of the coating. The line corresponding to the (101) direction becomes more intense, while the (100) and (102) peaks decrease in height. At the same time, a new peak appears, corresponding to the (112) orientation, that can be attributed to the presence of $\text{CeO}_2\cdot\text{ZrO}_2$ [23].

Electrochemical corrosion measurements

Open circuit potential

As it can be observed from Table 1, the open circuit potential values of the investigated samples recorded after one hour of immersion in the corrosive medium are relatively close to each other, with a variation of ± 30 mV. The shifts towards a more negative potential in the presence of nanoparticles in the Zn deposit suggest the existence of an influence exerted by these particles on the oxygen reduction process.

Table 1. Open circuit potential values for the obtained Zn and Zn-composite deposits

Deposit	Nanoparticles concentration [g L ⁻¹]	OCP [mV vs Ag/AgCl]
Zn	0	-983
Zn-ZrO ₂	1.25	-1014
Zn-CeO ₂		-1011
Zn-CeO ₂ ·ZrO ₂	1.25	-996
	5	-1008
Zn-CeO ₂ +ZrO ₂	1.25	-984
	5	-994

Polarization curves

The results of OCP analysis were further endorsed by conducting polarization studies. The cathodic and anodic polarization curves of Zn, Zn-(CeO₂·ZrO₂), Zn-(CeO₂+ZrO₂), Zn-ZrO₂ and Zn-CeO₂ coatings recorded after 1h of immersion in Na₂SO₄ solution (pH 5) are presented in Figure 4. From the polarization curves, the corrosion parameters were evaluated by using only the anodic Tafel slopes, due to the fact that the cathodic branches of the polarization curves are flat (the cathodic process is controlled by the diffusion of O₂, being impossible to calculate β_c). Thus, some degree of imprecision must be associated with the estimated corrosion rate under these conditions. However, a comparison between the behaviours of different deposits could be made, at least semi-quantitatively.

It has been established that a very low concentration of nanoparticles could be insufficient to enhance the corrosion resistance of the deposit, due to a too low percentage of nanoparticles embedded in the metallic matrix, while a too high concentration could generate defects in the coating, which can be starting points for generalized corrosion. Thus, an optimal concentration is required to be found for every particular system.

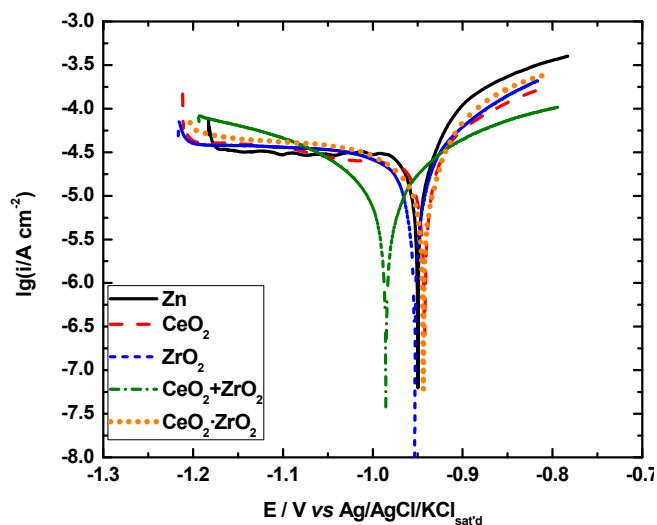


Figure 4. Polarization curves (± 200 mV vs OCP) for Zn and composite zinc deposits with a 1.25 g L^{-1} concentration of nanoparticles

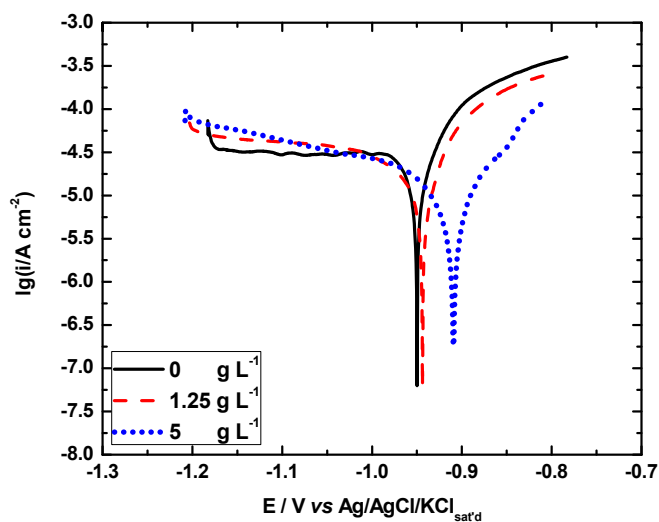


Figure 5. Polarization curves (± 200 mV vs OCP) for Zn and Zn- $\text{CeO}_2 \cdot \text{ZrO}_2$ deposits with various concentrations of nanoparticles

The kinetic parameters for the corrosion process were estimated and are presented in Table 2.

Table 2. Corrosion parameters estimated from potentiodynamic measurements for pure zinc deposit and for Zn–oxide nanoparticles composite coatings

Deposit	Nanoparticle concentration [g L ⁻¹]	i_{corr} [μ A cm ²]	E_{corr} [mV vs Ag/AgCl]	R_p [Ω cm ²]	R^2/N^*
Zn	0	65.76	-948	1272	0.99/17
Zn-ZrO ₂	1.25	27.03	-956	2679	0.99/25
Zn-CeO ₂		37.65	-942	1767	0.99/22
Zn-CeO ₂ -ZrO ₂	1.25	35.94	-944	2027	0.99/25
	5	10.60	-909	4542	0.99/27
Zn-CeO ₂ +ZrO ₂	1.25	15.40	-984	4063	0.99/23
	5	15.94	-953	3420	0.99/42

* N represents the number of points from which the R_p was estimated

The influence of the nanoparticles concentration on the corrosion behaviour of the composite coatings was already reported [2]. As it can be observed from Table 2, the lowest corrosion current density and the highest polarization resistance are noticed in the case when 5 g L⁻¹ binary CeO₂·ZrO₂ oxide nanoparticles were used.

In the case of the CeO₂+ZrO₂ mixture, the best corrosion resistance corresponded to 1.25 g L⁻¹ concentration, closely followed by the 5 g L⁻¹ concentration. At the same time, it should be mentioned that in this case, the cathodic branches of the polarization curves recorded when the mixture is used, becomes mostly controlled by the charge transfer step, instead of the O₂ diffusion step.

At a concentration of 1.25 g L⁻¹ the most beneficial effect was noticed in the case of CeO₂+ZrO₂ mixture, followed by ZrO₂ and the binary CeO₂·ZrO₂ oxide, confirming the importance of the nature and properties of nanoparticles (size, surface charge, shape, previous treatments etc.) in the corrosion behavior of the composite deposits in which the nanoparticles are incorporated [24]. At the same time, by comparing the results obtained when CeO₂ and ZrO₂ were used separately, with those obtained in the presence of their mixture, it can be observed that a synergistic effect occurs when both are present, suggesting that the zirconia nanoparticles in combination with ceria offers a better protection than each type of nanoparticles used alone, both having a complementary role in this process.

CONCLUSIONS

The analysis of the results led to the following conclusions:

- The co-deposition of oxide nanoparticles with zinc leads to changes in the morphology of the resulting nanocomposite coatings as compared to pure Zn coatings. The composite coatings incorporating binary $\text{CeO}_2\cdot\text{ZrO}_2$ oxides exhibited the highest corrosion resistance, due to the inclusion of the binary oxide in the metallic matrix.
- The physical and electrochemical properties of Zn coatings were best when the binary $\text{CeO}_2\cdot\text{ZrO}_2$ and $\text{CeO}_2+\text{ZrO}_2$ mixture oxide nanoparticles were used. CeO_2 provides enhanced corrosion protection, with an effect on the oxygen reduction reaction, while ZrO_2 inhibits the corrosion process, and improves the wear resistance.
- The binary oxides used in optimal concentration (5 g L^{-1}) were proven to be more efficient than the simple mixture of the two oxides (CeO_2 and ZrO_2) probably due to the uniform distribution of Ce and Zr oxides on the surface of the composite samples (50:50 w:w).
- A synergistic effect was put in evidence when the two oxides were used in mixture as compared to individual ones.
- The corrosion properties of the composite coatings depend on the nanoparticles concentration in the plating bath. Thus, an optimal concentration was put on evidence for the investigated nanocomposite deposits. The existence of an optimal concentration of nanoparticles is the result of the action of two contrary effects: on one hand, the nanoparticles have a beneficial influence, by reducing the active surface in contact with the corrosive medium and on the other hand, at a concentration that may be too high, they could generate defects in the metallic coating, stimulating corrosion.

EXPERIMENTAL SECTION

Materials

Three types of nanoparticles were used: ZrO_2 (Zirconium (IV) Oxide, Sigma Aldrich, TEM size $<100 \text{ nm}$), CeO_2 (Cerium (IV) Oxide, Sigma Aldrich (BET size $<25 \text{ nm}$) and a binary oxide $\text{CeO}_2\cdot\text{ZrO}_2$ (Sigma Aldrich, BET size $<50 \text{ nm}$). Also, experiments were performed using a physical mixture of commercial ZrO_2 and CeO_2 (50:50 w:w). In all experiments, the total concentration of nanoparticles (ZrO_2 , CeO_2 , $\text{CeO}_2\cdot\text{ZrO}_2$ and a mixture of the oxide nanoparticles ZrO_2 and CeO_2 (50:50 w:w) in the electrolytic bath, was 1.25 g L^{-1} , respectively 5 g L^{-1} . The particles were suspended in an aqueous solution ($\text{pH}=5.9$) containing $75 \text{ g L}^{-1} \text{ ZnCl}_2$, $230 \text{ g L}^{-1} \text{ KCl}$, $20 \text{ g L}^{-1} \text{ H}_3\text{BO}_3$,

and two additives (a surfactant and a brightening agent), 1 mL L⁻¹ each. The corrosion studies were carried out by using a solution of 0.2 g L⁻¹ Na₂SO₄, pH=5. All other reagents were of analytical grade and used as received.

Methods

Zn and Zn-oxide nanoparticles coatings were galvanostatically deposited on carbon steel (EN 10025 Euronorm) in a shape of a disc ($S = 0.5024 \text{ cm}^2$) at a current density of 20 mA cm⁻², during 30 minutes, under magnetic stirring at 250 rpm, by using a potentiostat (PARSTAT 2273), at room temperature ($21 \pm 2^\circ\text{C}$). The thickness of the resulting coatings was about 20 μm . Prior to the electrodeposition process, the working electrode was wet polished on emery paper of different granulations (from 600 to 2500) and finally on felt with a 2 μm diamond polishing paste (Buehler, US).

Before plating, the electrode was ultrasonicated for 2 min in ethanol, then thoroughly rinsed with ethanol and distilled water in order to remove any remaining impurities from the surface.

The 50 mL electrolytic bath containing the dispersed nanoparticles was ultrasonicated for 30 minutes then stirred at 400 rpm for 3 hours, previous to the plating procedure [17-19].

The electrodeposition experiments were performed in a three-electrode cell with a volume of 62 mL, with a separate compartment for the reference electrode connected with the main compartment *via* a Luggin capillary. The working electrode was the coated steel disc, the reference electrode was an Ag/AgCl/KCl_s electrode and the counter electrode was a platinum coil.

During corrosion tests, the potentiodynamic polarization measurements were conducted using an electrochemical analyzer (PARSTAT 2273).

Corrosion experiments were carried out in 0.2 g L⁻¹ aerated Na₂SO₄ solution (pH 5), at room temperature. Open-circuit potential (OCP) measurements were performed as a function of time. Anodic and cathodic polarization curves were recorded in a potential range of $E = E_{\text{corr}} \pm 200 \text{ mV}$, with a scan rate of 0.166 mV s⁻¹.

The structure of the deposits and the preferred orientation of the crystallites were determined by XRD analysis with a Brucker X-ray diffractometer with a Cu K α ($\lambda = 0.15406 \text{ nm}$) at 45 kV and 40 mA. The 2θ range of 20–100° was recorded at the rate of 0.02° and 2θ 0.5 s⁻¹. The crystal phases were identified comparing the 2θ values and intensities of reflections on X-ray diffractograms with JCP data base using a Diffrac AT-Brucker program.

The SEM micrographs of the surfaces were performed by using a Carl Zeiss Evo series 40x VP and the EDX interpretations were obtained by using an Oxford Instruments EDX equipment, coupled with SEM.

ACKNOWLEDGEMENTS

This work was possible with the financial support of the Sectoral Operational Programme for Human Resources Development 2007–2013, co-financed by the European Social Fund, under the project number **POSDRU/107/1.5/S/76841** with the title „Modern Doctoral Studies: Internationalization and Interdisciplinarity”.

Prof. Dr. Lorenzo Fedrizzi and Dr. Maria Lekka from the University of Udine, Italy are gratefully acknowledged for the SEM and EDX observations.

Dr. Emil Indrea from the National Institute for Research and Development of Isotopic and Molecular Technologies Cluj-Napoca, Romania, is gratefully acknowledged for the XRD measurements.

REFERENCES

- [1] A. Hovestad, L.J.J. Jansen, *Journal of Applied Electrochemistry*, **1995**, 25, 519.
- [2] C.T.J. Low, R.G.A. Wills, F.C. Walsh, *Surface & Coatings Technology*, **2006**, 201, 371.
- [3] A. Gomes, M.I. Da Silva Pereira, M.H. Mendonça, F.M. Costa, *Journal of Solid State Electrochemistry*, **2005**, 9, 190.
- [4] B.M. Praveen, T.V. Venkatesha, *Applied Surface Science*, **2008**, 254, 2418.
- [5] W. Liu, Y. Chen, C. Ye, P. Zhang, *Ceramics International*, **2002**, 28, 349.
- [6] P.M. Ashraf, S.M.A. Shibli, *Electrochemistry Communications*, **2007**, 9, 443.
- [7] T.T. Tuaweri, G.D. Wilcox, *Surface & Coatings Technology*, **2006**, 200, 5921.
- [8] K. Kondo, A. Ohgishi, Z. Tanaka, *Journal of The Electrochemical Society*, **2000**, 147, 2611.
- [9] H.M. Hawthorne, A. Neville, T. Troczynski, X. Hu, M. Thammachart, Y. Xie, J. Fu, Q. Yang, *Surface & Coatings Technology*, **2004**, 176, 243.
- [10] Y. Wang, R. Kovacevic, J. Liu, *Wear*, **1998**, 221, 47.
- [11] S.K. Yen, M.J. Guo, H.Z. Zan, *Biomaterials*, **2001**, 22, 125.
- [12] J.H. Sui, W. Cai, *Nuclear Instruments and Methods in Physics Research B*, **2006**, 251, 402.
- [13] Y-P. Fu, S-H. Hu, B-L. Liu, *Ceramics International*, **2009**, 35, 3005.
- [14] F. Hou, W. Wang, H. Guo, *Applied Surface Science*, **2006**, 252, 3812.
- [15] K. Vathsala, T.V. Venkatesha, *Applied Surface Science*, **2011**, 257, 8929.
- [16] A.V. Pop, A. Vlasa, S. Varvara, C. Bulea, L. Muresan, *Optoelectronics and Advanced Materials*, **2009**, 3, 1290.
- [17] A. Vlasa, S. Varvara, A. Pop, C. Bulea, L. M. Muresan, *Journal of Applied Electrochemistry*, **2010**, 40, 1519.
- [18] E. Grünwald, C. Bulea, “Electrodepunerea zincului si aliajelor de zinc din solutii slab acide”, Ed. Casa Cartii de Stiinta, Cluj-Napoca, **2011**, 211.

- [19] P. Nemes, M. Zaharescu, L. M. Muresan, *Journal of Solid State Electrochemistry*, **2012**, DOI 10.1007/s10008-012-1901-6.
- [20] S.T. Aruna, C.N. Bindu, V. Ezhil Selvi, V.K. William Grips, K.S. Rajam, *Surface & Coatings Technology*, **2006**, 200, 6871.
- [21] M.F. Montemor, W. Trabelsi, S.V. Lamakac, K.A. Yasakauc, M.L. Zheludkevichc, A.C. Bastos, M.G.S. Ferreira, *Electrochimica Acta*, **2008**, 53, 5913.
- [22] S. Ranganatha, T.V. Venkatesha, K. Vathsala, M.K. Punith Kumar, *Surface & Coatings Technology*, **2012**, 208, 64.
- [23] F. Zhang, C.H. Chen, J.M. Raitano, J.C. Hanson, W.A. Caliebe, S. Khalid, S.W. Chan, *Journal of Applied Physics*, **2006**, 99, 084313.
- [24] C. Zanella, M. Lekka, P.L. Bonora, *Journal of Applied Electrochemistry*, **2009**, 39, 31.